Array-Controlled Ultrasonic Manipulation of Particles in Planar Acoustic Resonator

Peter Glynne-Jones, Christine E. M. Démoré, *Member, IEEE*, Congwei Ye, Yongqiang Qiu, *Student Member, IEEE*, Sandy Cochran, *Member, IEEE*, and Martyn Hill

***Abstract*—Ultrasonic particle manipulation tools have many promising applications in life sciences, expanding on the capabilities of current manipulation technologies. In this paper, the ultrasonic manipulation of particles and cells along a microfluidic channel with a piezoelectric array is demonstrated. An array integrated into a planar multilayer resonator structure drives particles toward the pressure nodal plane along the centerline of the channel, then toward the acoustic velocity maximum centered above the subset of elements that are active. Switching the active elements along the array moves trapped particles along the microfluidic channel. A 12-element 1-D array coupled to a rectangular capillary has been modeled and fabricated for experimental testing. The device has a 300-μm-thick channel for a half-wavelength resonance near 2.5 MHz, with 500 μm element pitch. Simulation and experiment confirm the expected trapping of particles at the center of the channel and above the set of active elements. Experiments demonstrated the feasibility of controlling the position of particles along the length of the channel by switching the active array elements.**

I. Introduction

The ability to hold and reposition cells using particle manipulation technologies is now established as an important factor in many significant advances in life sciences research [1], [2]. Optical tweezers have been the major technology used to date; however, ultrasonic radiation forces offer several potential advantages, including the ability to move larger particles or cells and groups of particles and cells in the range from 1 μm to hundreds of micrometers. It is also potentially simpler and cheaper to implement ultrasonic manipulation in a life sciences laboratory-based device incorporating microfluidics than to implement optical tweezing technology.

The frequencies typically employed in ultrasonic manipulation in liquids range from around 500 kHz to a few tens of megahertz, although frequencies of 100 MHz have been reported [3]. For resonant ultrasonic devices, an ultrasound standing wave is set up within a fluid chamber, creating a pressure node at which particles can be trapped. A typical multilayer ultrasonic resonator configuration is illustrated in Fig. 1. The thickness of the fluid chamber is close to a half-wavelength at an operating frequency in the megahertz range [4], thus leading to devices compatible with microfluidic dimensions and technologies. Planar resonators with lateral dimensions much larger than a wavelength can be used, permitting control over larger domains, and making these planar devices suitable for levitating and concentrating particles in a fluid flow.

A range of applications employing the levitating and concentrating properties of ultrasonic standing waves have been demonstrated, including cell medium exchange and washing [5]; enhanced agglutination assays [6]; bioreactors and cell culture of suspended colonies [7]; cell sorting, such as separating red blood cells from plasma [8], removing lipids from blood for recycling during cardiac surgery [9], extraction and concentration of pathogen spores for biodetection [10], and manipulation of spores toward surfaces for enhanced detector sensitivities [11]; sheath-free cell focusing for flow cytometry [12]; and cell interaction studies [13]. Despite the ability to lyse [14] or sonoporate [15] cells at higher sound intensities, the manipulation of cells with ultrasound standing waves at reasonable excitation levels has been shown to be compatible with continued cell viability and proliferation in several studies [16]–[20]. More fine-grained control over particle positions has been limited because of the dominant effect of chamber geometry on resonant modes. A range of techniques has been demonstrated to overcome this limitation, including frequency sweeping [21], mode switching/mixing [22], [23] and the use of two or more transducers to modulate the standing wave field [24], [25]. However, most of these techniques have been limited to manipulation along a single dimension, in the direction of wave propagation.

The electronic sonotweezer presented in this paper demonstrates the potential of using an electronically controlled array with a multilayer resonator to move particles within a chamber. Although the device described here uses a 1-dimensional array, the approach has the potential to be expanded for 2-D planar manipulation. The concept is similar to that demonstrated by Kozuka *et al.* [26], in which an array of line-focused elements transported particles laterally. This work extends that concept to planar resonators, miniaturizes it, and explores in some detail the mode of operation of the device through finite element modeling and experimental verification.

The principle of operation is shown in Fig. 1. Potential and kinetic energy density gradients, which generate the forces on cells, are formed within the fluid channel between a transducer and a reflector layer because of the ultrasound standing wave produced in the device structure

Manuscript received June 16, 2011; accepted February 18, 2012. This work has been funded by the Engineering and Physical Sciences Research Council, UK, through the Sonotweezers project.

P. Glynne-Jones, C. Ye, and M. Hill are with the School of Engineering Sciences, University of Southampton, Southampton, UK.

C. Démoré, Y. Qiu, and S. Cochran are with the Institute for Medical Science and Technology, University of Dundee, Dundee, UK (e-mail: cdemore@ieee.org).

DOI http://dx.doi.org/10.1109/TUFFC.2012.2316

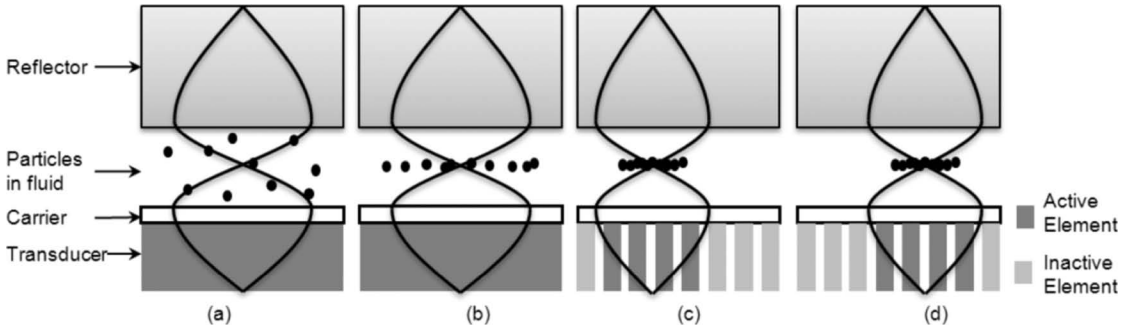

Fig. 1. Acoustic particle manipulation with an array-controlled multilayer resonator. (a) A standing wave is generated through the thickness of the structure and (b) particles in the fluid layer move toward the pressure node plane. (c) Lateral acoustic energy density gradients resulting from the finite source width trap particles above active array elements. (d) Switching active array elements moves the lateral trapping position so particles are moved along the fluid channel.

[27]. The locations of pressure and acoustic particle velocity minima and maxima, and consequently the respective potential and kinetic energy density minima and maxima in the fluid layer are dictated by the layer thicknesses and materials, as well as the transducer width and driving frequency. The force on particles or cells is dependent both on the acoustic energy gradients and on the size and acoustic properties of the particle.

Lateral trapping can be accomplished with an array in place of a single planar transducer, by driving a subset of the elements [Fig. 1(c)]. A lateral gradient in the kinetic energy density is produced by the finite source width, and particles are trapped above the center of the active elements. The subset of array elements can then be switched to move the active region along the device to shift the trap location and move particles along the length of the channel [Fig. 1(d)]. A 1-D array integrated into a planar resonator, therefore, provides control of both vertical and lateral forces for trapping and moving particles within a fluidic channel.

The theoretical background to vertical and lateral trapping in an ultrasound standing wave device is considered in the next section. Then the design of the array-controlled multilayer resonator is presented, followed by simulation of device performance and trapping forces. Finally, the device fabrication and experimental demonstration of trapping and manipulation in the ultrasonic resonator are presented.

II. Theory

Acoustic radiation forces are a non-linear effect. In a linear acoustic model, a particle within an acoustic field experiences an oscillatory force resulting from the acoustic pressure variations, but this averages to zero. However, if second-order terms are included in the model and a time average of the pressure on the particle surface is taken, a nonzero average force is found to exist; this is the acoustic radiation force.

The radiation force exerted on an incompressible sphere was calculated by King [28]. Yosioka and Kawasima [29] extended this calculation to the case of a compressible sphere with a small diameter in comparison with the acoustic wavelength within a planar field. Gor'kov [30] then generalized it to the case of an arbitrary standing wave field, expressing by the time-averaged force, F, as a function of the gradients of the time-averaged kinetic and potential energy densities of the standing wave field:

$$F = -\nabla\left(\left(1 - \frac{\rho_{\mathrm{f}} c_{\mathrm{f}}^2}{\rho_{\mathrm{p}} c_{\mathrm{p}}^2}\right)\langle E_{\mathrm{pot}}\rangle - \left(\frac{3(\rho_{\mathrm{p}} - \rho_{\mathrm{f}})}{(2\rho_{\mathrm{p}} + \rho_{\mathrm{f}})}\right)\langle E_{\mathrm{kin}}\rangle\right)V, \quad (1)$$

where V is the particle volume, ρ_{f} and ρ_{p} are the densities of the fluid and particle respectively, and c_{f} and c_{p} are the speeds of sound in the fluid and particle. The time-averaged kinetic and potential energy densities are related to the acoustic pressure field p and acoustic velocity magnitude u by

$$E_{\mathrm{pot}} = \frac{1}{2\rho_{\mathrm{f}} c_{\mathrm{f}}^2} p^2, \quad (2)$$

$$E_{\mathrm{kin}} = \frac{1}{2}\rho_{\mathrm{f}} u^2. \quad (3)$$

Hence, a particle that is less compressible than the fluid will experience a component of force toward the potential energy density minimum and a particle that is denser than its surrounding fluid will experience a component of force toward the kinetic energy density maximum.

In many applications, the particles of interest, e.g., polystyrene beads or biological cells, experience a larger contribution from the potential energy term than from the kinetic term [determined by inserting reasonable estimates for particle properties into (1)–(3)]. Thus, particle behavior is, to a first approximation, predictable from the pressure field within a device. Consider the resonant acoustic field depicted in Fig. 2, in which a transducer is coupled to the base of a fluid chamber with a reflector above. A resonance is formed over the half-wavelength thickness of the chamber, with a stronger field near the center. The gradient in energy density in the width of the chamber can be caused either by a transducer which is small relative to the lateral channel dimensions or by a non-rectangular

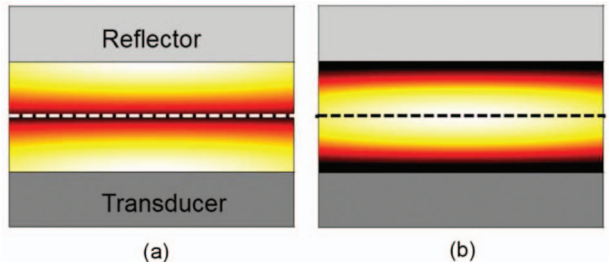

Fig. 2. Example of acoustic field distributions: (a) pressure magnitude and (b) velocity magnitude, in a resonant cavity, with a stronger field near the center of the cavity. Arbitrary linear scale: light: 1, dark: 0.

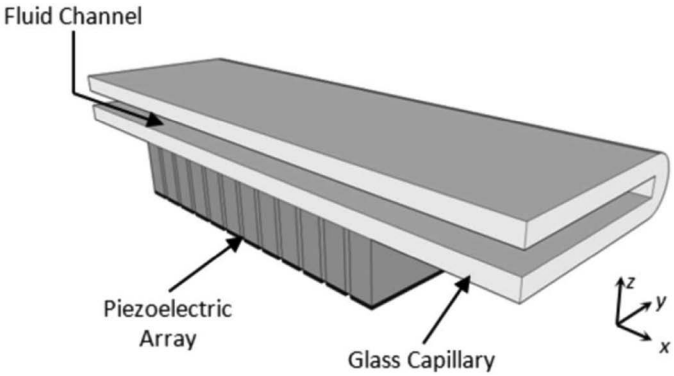

Fig. 3. Cross-section of multilayer resonator with capillary coupled to a 1-D array. Capillary flow direction is along the x-axis.

channel, as shown by Hammarström *et al.* [31]. The potential energy terms of (1) mean that particles in all locations in the chamber are driven toward the pressure nodal plane on the centerline, shown as a broken line. Once particles reach the pressure nodal plane, there is no further contribution from the potential energy terms, because there is zero gradient along this centerline. The kinetic energy term provides an additional, but typically smaller force, and, because of the negative sign of the kinetic energy term compared with the potential term in (1), particles are drawn toward the center point of the chamber, where the velocity field amplitude is at a maximum. The kinetic energy contribution explains the trapping and lateral agglomeration seen in many planar resonators, e.g., [31], [32], although in some cases there may also be a pressure contribution to lateral trapping. The force resulting from the kinetic energy density gradient is the basis for the electronically controlled manipulation device presented in this paper.

III. Design and Modeling

A. Device Configuration

The device chosen to demonstrate the feasibility of controlled lateral manipulation with an array is based upon the structure of a multilayer planar resonator, with a fluid channel above a transducer. Through appropriate choices of layer thickness, there are several possible modes [33], moving particles to various heights within the channel. Here we choose a half-wave design, i.e., with a half-wavelength thick fluid layer, in which vertical forces move particles to a pressure nodal plane along the centerline of the channel. Such devices are relatively insensitive to suboptimal layer thicknesses because of the strong reflections found at the fluid layer boundaries.

The chosen device configuration is illustrated in Fig. 3. A glass capillary with a rectangular cross section is coupled to a 1-mm-thick plate containing the 1-D array. The capillary forms the fluid channel and top reflector; the bottom of the capillary is a carrier or isolation layer between the transducer and the fluid layer. The disposable capillaries are simple to use, highly resonant, and point to the possibility of creating disposable, sterile chambers for use in life-science applications [31]. The capillary (Vitri-Com, Ilkley, UK) has a 300 μm channel thickness, corresponding to a 2.52 MHz half-wavelength resonance, and 300 μm wall thickness.

The array element pitch determines the step size for moving agglomerations of particles along the channel; a finer pitch would give more precise positional control. The pitch must be small enough such that when the acoustic field is shifted along the channel, the kinetic energy density has only a monotonic increase between the original and the new trapping locations. For the present simulations and experiments, the pitch is set at 500 μm, less than half the distance between the main trapping location and subsidiary traps that can arise in the capillary, as will be discussed further.

A kerfless array configuration, in which the elements are defined by the electrode pattern on a bulk piezoelectric plate and not physically separated by a kerf, has been developed. The kerfless array design greatly simplifies the fabrication, and consequently the cost, of the device [34], [35], and makes integration with the capillary or other resonant channels straightforward. Although the lateral extent of the active area in the channel increases because of electrical field fringing in the kerfless array and mechanical coupling along the piezoelectric plate and the resonant structure, the operation of the device is not significantly limited. Simplifying the fabrication is a particularly worthwhile consideration in applications for which low-cost devices are required and the larger effective element size does not constrain the operation of the device.

B. One-Dimensional Modeling

A one-dimensional transfer impedance model [36] was used to optimize the transducer layer thickness for the given capillary dimensions. The one-dimensional model treats the device as an ideal planar structure with plane waves traveling only in the thickness direction; still, it is sufficiently accurate to identify promising combinations of layer thickness in planar resonators. The model parameters are listed in Table I; the lead zirconate titanate (PZT) used for the transducer layer is PZ26 (Ferroperm

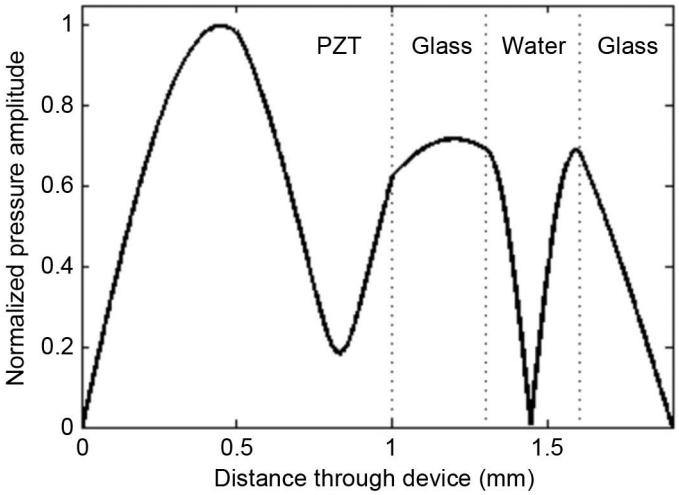

Fig. 4. Normalized pressure distribution through the thickness of the device from 1-D simulation.

Piezoceramics, Kvistgaard, Denmark). Fig. 4 shows the modeled pressure distribution through the layers at the 2.52-MHz resonance. It can be seen that although the capillary wall thicknesses are not optimum for a half-wave design, a strong resonance is predicted in the fluid layer. The pressure minimum and the resulting trapping position is 144 μm from the lower surface of the fluid channel.

C. Finite Element Analysis

1) Model Configuration: The operation of the device has also been modeled using finite element analysis (FEA; Comsol Multiphysics, Comsol Ltd., Hertfordshire, UK) to include the effects of lateral acoustic field gradients and array geometry. A 2-D slice through the structure along the length of the capillary has been created. This approximates the structure as infinite in the y-direction to reduce computational complexity. The model includes piezoelectric, linear elastic, and linear acoustic domains coupled together, modeling the full interaction from excitation voltage through to acoustic resonance. The resulting linear acoustic results are used in conjunction with (1) to calculate radiation forces on a typical particle (see Table I). The structure modeled is illustrated in Fig. 5; material properties are the same as the 1-D simulation, listed in Table I. The elements, defined by the electrode position on the PZT plate are positioned with a 0.5-mm pitch, and the total channel length is 16 mm. Free-field boundary conditions are specified along the top and bottom surfaces of the device and at the edges of the PZT layer because the device operates in air. Because only a section of the capillary is modeled, radiation boundary conditions were applied at the lateral edges of the fluid layer to absorb acoustic energy incident at the boundary. This approximation is reasonable for the current configuration because the capillary is much longer than the array, and energy in the fluid layer traveling away from the array will be coupled into the solid layers and absorbed. The loss within the system is difficult to quantify, because much of it is caused by energy coupled out of the system through the clamping to maintain contact between the capillary and array. Q-factors of 50 were applied to all materials in the model; this provides a reasonable match to the experimental results. A mesh dependency study was performed and a mesh size of $\lambda/20$, where λ is the longitudinal acoustic wavelength in each respective material, was found to be sufficient. At this density, a computational time of around 5 min was required for harmonic analysis of the model over a set of 100 frequency points (computer: Latitude E4310, Dell Inc., Round Rock, TX). The frequency of maximum energy density in the fluid, i.e., the resonance frequency, was determined with harmonic analysis of the model. The potential and kinetic energy densities within the fluid layer at the resonance frequency were calculated and the distributions analyzed to calculate the forces on a typical particle.

The energy density in the fluid layer was found to be maximal at 2.53 MHz, very close to the resonance frequency calculated from the 1-D model. The simulated spatial distributions of potential and kinetic energy densities in the fluid layer are shown in Fig. 6. Pairs of active elements in the kerfless array, indicated by the shaded elements, were driven with 17 V_{pp}, corresponding to maximum loaded amplitude on the signal generator described subsequently. The simulations clearly indicate a trapping position, at the potential energy density minimum and kinetic energy density maximum, near the channel center line and centered above the active elements. The region of high kinetic energy density extends beyond the edges of the excited region because of electrical field fringing in the piezoelectric ceramic, and spreading of the acoustic energy in the resonant structure, which leads to the subsidiary trapping sites discussed in subsequently.

2) FEA Results: The force on a 10-μm polystyrene sphere was calculated from the energy density distributions using (1). The calculated vertical force in the chan-

TABLE I. MODELED PROPERTIES AND LAYER DIMENSIONS.

Layer	Material	Density (kg/m^3)	Speed of sound (m/s)	Thickness (μm)
Reflector	Glass	2500	5872	300
Fluid	Water	1000	1485	300
Carrier	Glass	2500	5872	300
Transducer	PZT (PZ26)	7700	4076	1000
Particle	Polystyrene	1055	1962	Diameter 10

PZT = lead zirconate titanate.

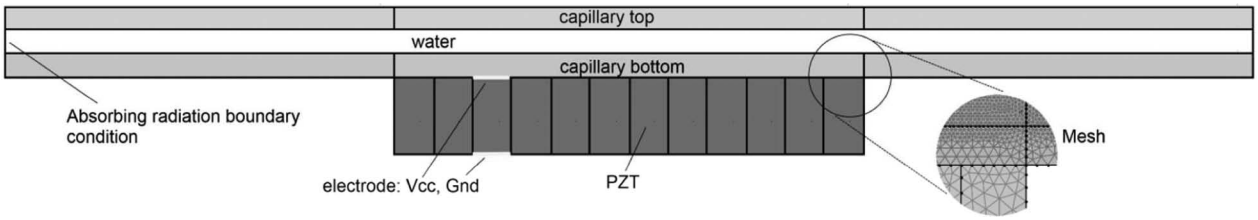

Fig. 5. Diagram of 2-D finite element analysis model of capillary coupled to kerfless 1-D array.

nel thickness above the middle of the active elements and the calculated lateral force along the channel at the height of the pressure node above the active elements are shown in Fig. 7. The calculated maximum vertical and lateral forces are 206 and 2.3 pN, respectively. As expected, the ratio of the vertical to lateral force indicates that the force on a particle is dominated by the potential energy density gradient, and therefore the pressure distribution.

It can be seen in Fig. 7(b) that the trapping location for the lateral force (indicated by circles) moves along the channel, staying close to the center of the active electrodes. The nature of the resonance means that subsidiary trapping sites are also possible, for example, at 0.5 mm from the edge of the array with elements 5 and 6 active. This has the potential to limit the extent over which the trap is effective, and has important implications for the minimum pitch of the electrodes. If the pitch is too large, particles may be drawn to a subsidiary trapping point if that is closer than the primary trapping point when the active electrodes are switched along the array. With the current design, the distance to the subsidiary trapping position is much larger than the array pitch. Although the lateral trapping force profile is not as smooth as the vertical force profile, it is sufficient for manipulating particles to the kinetic energy density maximum. The subsidiary traps potentially originate from three separate effects: 1) Transducer geometry edge effects, 2) flexural waves in the capillary surface exciting competing resonances, and 3) lateral acoustic modes in the fluid in the length and width direction. Examining the FEA model, 1) and 2) can be seen, and 3) is not obvious because the chosen boundary conditions will tend to suppress this effect.

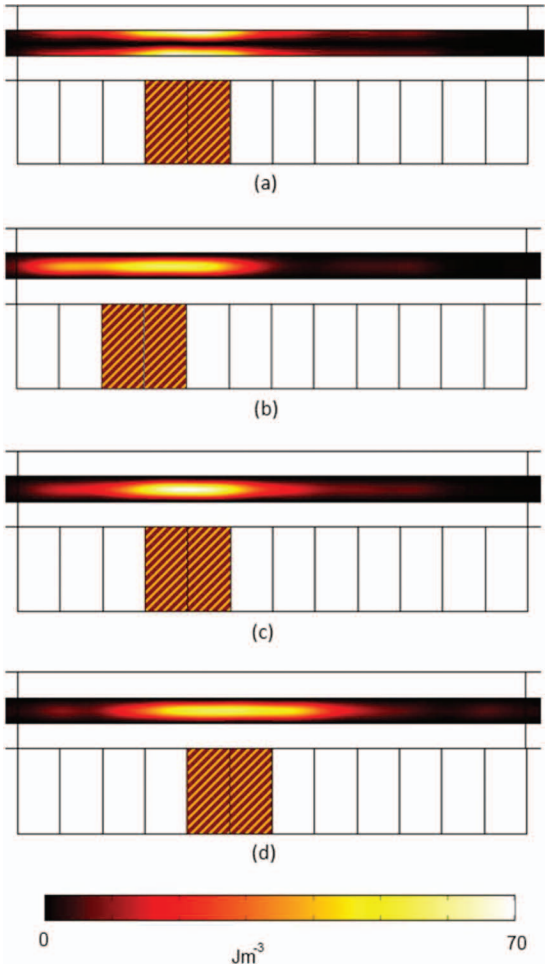

Fig. 6. Calculated spatial distributions in the fluid channel of (a) potential energy density and (b)–(d) kinetic energy density at resonance. Shading on elements indicates which elements are active.

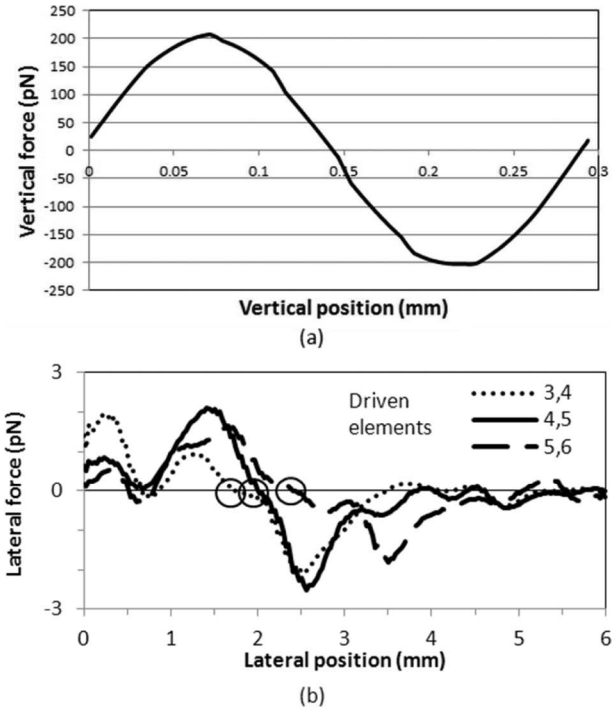

Fig. 7. Forces calculated from finite element analysis for a 10-μm polystyrene bead in the fluid channel. (a) Vertical force in channel thickness above the middle of active elements 4 and 5. (b) Lateral forces along the center line of the fluid channel for the listed active elements. Circles indicate the primary trapping position for each case.

IV. Experimental Evaluation

A multilayer resonator with a 12-element array has been fabricated to experimentally demonstrate the feasibility of controlled manipulation of particles along a microfluidic channel. A glass capillary was coupled to a kerfless 1-D array with 500-μm-pitch elements defined by the electrode pattern on the surface of a piezoelectric ceramic plate embedded in an epoxy plate. By exciting different sets of elements, trapping sites could be set up along the channel to trap and then move an agglomerate of 10-μm polystyrene beads.

A. Device Fabrication

A schematic diagram of the kerfless array fabrication process is shown in Fig. 8. A 6 × 4 mm PZT plate was embedded in an epoxy plate to form the base of the multilayer resonator and to position the array within the chamber housing. The epoxy (Epofix, Struers Ltd., Rotherham, UK) was loaded with glass microbubbles (3M United Kingdom PLC, Bracknell, UK) to inhibit wave propagation within the epoxy; this was cast over the PZT plate. The transducer and epoxy wafer were lapped to the specified 1-mm thickness with a precision lapping and polishing machine (PM5, Logitech Ltd., Glasgow, UK), exposing the piezoelectric ceramic on both the top and bottom surfaces of the wafer. After applying silver paint electrodes, a printed circuit board (PCB) with 12 signal tracks and a ground track was fixed to the back of the wafer and aligned with the 6-mm edge of the ceramic plate. Conductive epoxy was used to connect the transducer electrode with the conductive tracks on the PCB and the PCB was thinned to minimize the amount of conductive epoxy required to make the electrical connection. A high-precision dicing saw (MicroAce 66, Loadpoint Ltd., Swindon, UK) was used to scratch-dice simultaneously the ceramic, the conductive epoxy and the circuit board to separate the electrodes, defining the kerfless array elements. The ground electrode on the front face of the transducer was also connected to the PCB ground track with conductive epoxy. A 13-pin connector, to which driving circuitry was connected, was soldered onto the PCB. The fabricated array with PCB connector is shown in Fig. 9(a).

A rectangular glass capillary with 6.0 × 0.30 mm internal cross section was centered over the piezoceramic plate, with the fluid channel axis parallel to the length of the array. The capillary was coupled to the transducer plate with glycerol and the two components were clamped together in a chamber housing, shown in Fig. 9(b). The device layer thicknesses and materials are the same as those used in the simulations and detailed in Table I.

B. Experimental Results

A suspension of 10.3-μm-diameter green-fluorescent polystyrene beads (Polysciences Inc., Warrington, PA) in water was introduced in the capillary channel. A function generator (3320A, Agilent Technologies Inc., Santa Clara, CA) was connected to the array to drive two adjacent elements at the half-wave mode frequency at up to 17 V_{pp}. The fluorescent beads were observed in the capillary through an epifluorescence microscope. The primary resonance frequency was found by searching through a range of frequencies close to that predicted by modeling, and identifying the frequency which created the required trapping action, with beads drawn into a single agglomerate at the center of the channel above the active elements. Other resonance frequencies can also occur, corresponding to standing waves in the width of capillary, but these are avoided for the present measurements. A small shift of up to around 0.1 MHz about the expected 2.5 MHz half-wave mode frequency was observed when the capillary was replaced, because of different couplant thicknesses, or, more likely, variation in capillary dimensions [31], but otherwise the primary resonance frequency remained stable.

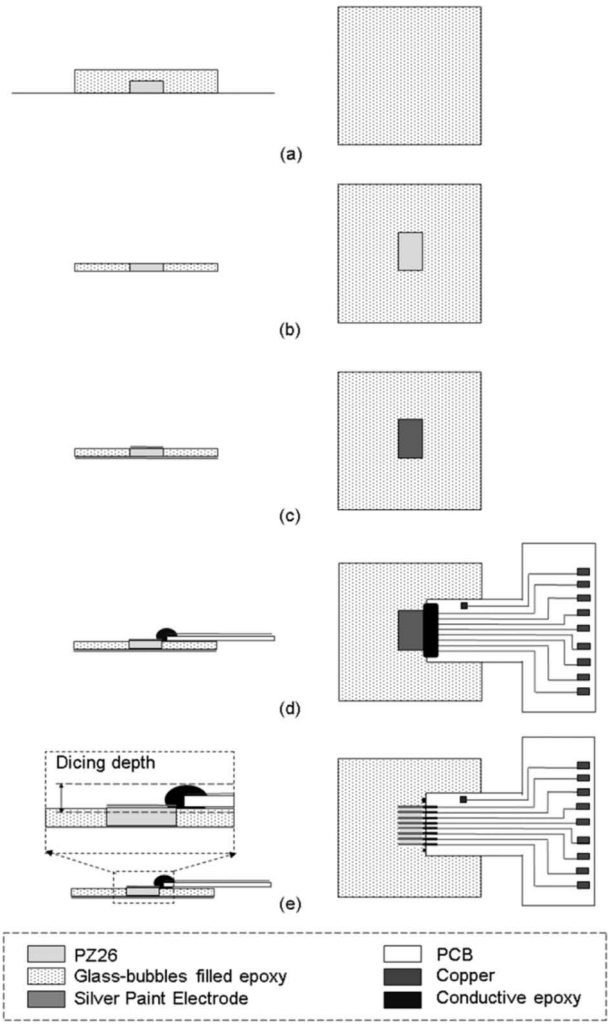

Fig. 8. Schematic diagram of array fabrication. (a) Glass-bubble-loaded epoxy is cast on a lead zirconate titanate plate and (b) lapped to thickness. (c) Electrodes are deposited on the plate surfaces and (d) connected to a printed circuit board (PCB) with conductive epoxy. (e) Elements are defined by scratch-dicing.

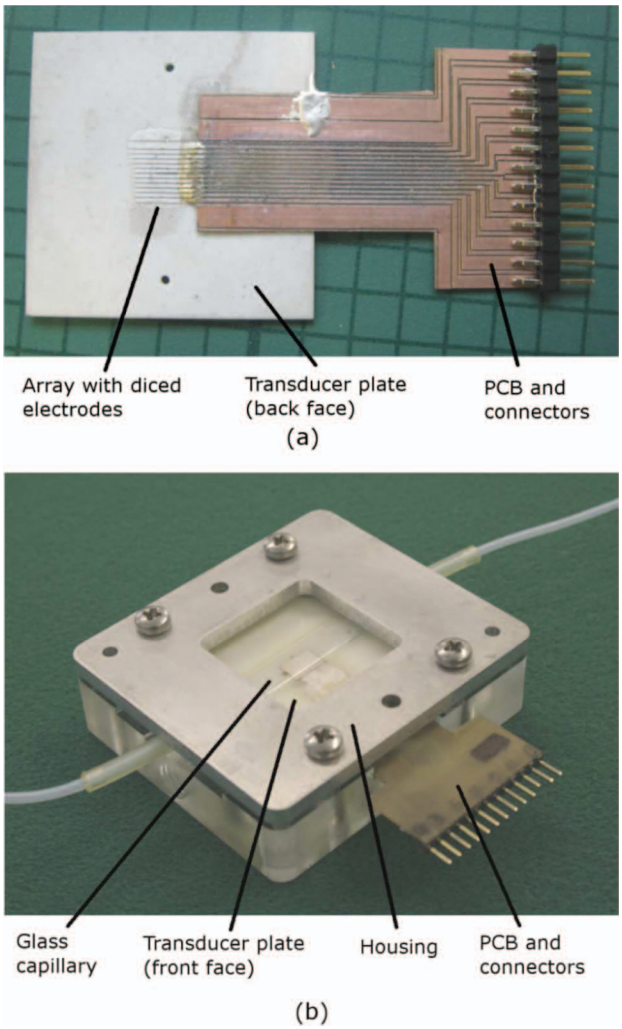

Fig. 9. (a) Back face of the fabricated array with printed circuit board (PCB) for electrical connections to elements and (b) in housing, coupled to the capillary fluidic channel.

When the driving signal was turned on to activate two adjacent elements, dispersed beads initially moved quickly in the vertical (z) direction to the centerline of the channel, then more slowly into an agglomerate centered above the active elements. Once the particles had agglomerated at the trapping point, the elements in the array were switched sequentially to move the kinetic energy density maximum along the fluid channel in the lateral (x) direction. Fig. 10 shows the bead agglomerate, approximately 500 μm long, translated along the channel after the connection to the active pair of electrodes had been stepped along the array, moving the electrical connection by hand. Throughout the manipulation experiments, the bead agglomerate could be moved smoothly and consistently in both forward and reverse directions ($\pm x$) along the channel. Very little leakage of particles from the agglomerate was observed, indicating that the trap is large enough to hold the agglomerate, and subsidiary trapping points do not interfere with the trapping.

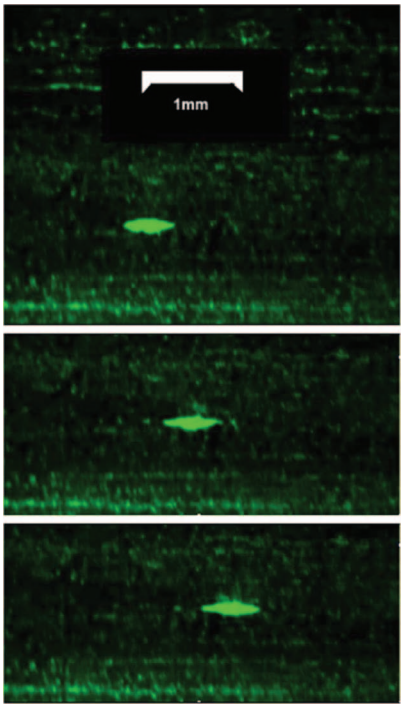

Fig. 10. Microscope images of a fluorescent polystyrene bead agglomerate moved along the length of the microfluidic channel.

The maximum vertical force on the beads was estimated by balancing against gravity and accounting for buoyancy. With a single bead trapped laterally, the driving voltage was reduced until the bead was no longer suspended in the fluid, determined visually by it dropping out of the ~10-μm-deep focal plane of a 50× microscope objective. Assuming a linear system, the pressure magnitude is proportional to the driving voltage, and therefore the force is proportional to the square of the applied voltage. The levitation force on the bead was balanced against gravity at 0.68 V_{pp}, corresponding to a levitation force of 180 ± 60 pN at 17 V_{pp} drive signal. The pressure amplitude in the device can be calculated from (1), substituting the material parameters given in Table I; at 17 V_{pp}, the pressure amplitude of the standing wave is 740 ± 130 kPa.

An estimate of the lateral trapping force on individual beads was obtained from the viscous drag force, F_d, arising from the particle velocity, which is given by Stoke's law,

$$F_d = 6\pi\mu r v, \tag{4}$$

where the viscosity of the water, $\mu = 1.002$ mN·s/m^2, r is the particle radius, and v is the particle velocity. This equation is valid because the Reynolds number of the flow is of the order 2×10^{-4}, and wall effects can be neglected because the beads are levitated by the half-wave resonance, with the nearest wall some 15 bead diameters away. The maximum particle velocity was found to be 0.016 mm/s, corresponding to $F_d = 1.6 \pm 0.3$ pN. The ratio of vertical levitation force to lateral force is 90, agreeing to within 10% with the results from FEA.

V. Conclusions

The feasibility of electronically controlled manipulation of particles and cells along a microfluidic channel has been investigated with both simulation and experiment. A 1-D array has been integrated into a multilayer ultrasonic resonator to both concentrate particles along the centerline of a microfluidic channel and move them back and forth along the length of the channel by switching the active elements along the array. A half-wave mode resonance in the thickness of the channel drives particles to the potential energy density minimum at the pressure nodal plane along the channel centerline. If the length of the active region in the array is shorter than the channel length, a lateral gradient in the acoustic particle velocity arises, and particles are drawn to the kinetic energy density maximum, centered above the active elements. Both experiment and modeling confirm the expected trapping, and experiments demonstrate the feasibility of manipulating particles and agglomerates with a 1-D array.

The prototype device presented comprises a rectangular glass capillary coupled to a 12-element 1-D array of switched transducer elements to generate an ultrasound standing wave above the active array elements. The 300 μm thickness of the capillary channel dictates a 2.5 MHz operating frequency for a half-wavelength mode in the fluid layer of the resonator. The 500 μm element pitch of the fabricated array is fine enough to consistently control the position of particles in the fluid channel. Although a finer pitch array would provide more precise control, and a longer array would limit edge effects resulting from the finite length of the array and add flexibility to the system, for example, by allowing two agglomerations to be manipulated simultaneously, the present device is sufficient to prove the principle of operation. Experiment and modeling also confirm that, although forces on representative particles such as 10-μm polystyrene beads are dominated by the pressure gradient in the field, the gradient in the acoustic particle velocity field is sufficient for lateral manipulation.

The initial results from the array-controlled multilayer resonator presented in this paper support further development of a new class of electronic sonotweezers for manipulation of cells and groups of cells. Optimization of the layers and array design for larger forces and more precise control of suspended particles and cells will enable life scientists to trap and manipulate cells or groups of cells at specific positions along a fluid channel for a broad range of experiments.

Acknowledgments

The authors thank D. Brennan of the University of Southampton, A. Anderson of the University of Dundee, the Microengineering and Biomaterial Research Group at the University of Dundee, Loadpoint Ltd. (Swindon, UK), PCT Ltd. (Aberdeen, UK), Logitech Ltd. (Old Kilpatrick, Glasgow, UK), and the Sonotweezers project partners at the Universities of Bristol and Glasgow for their support and assistance in this research.

References

[1] D. G. Grier, "A revolution in optical manipulation," *Nature*, vol. 424, pp. 810–816, Aug. 14, 2003.

[2] A. Neild, S. Oberti, and J. Dual, "Design, modeling and characterization of microfluidic devices for ultrasonic manipulation," *Sens. Actuators B*, vol. 121, no. 2, pp. 452–461, 2007.

[3] M. Takeuchi, H. Abe, and K. Yamanouchi, "Ultrasonic micromanipulation of small particles in liquid using VHF-range leaky wave transducers," in *IEEE Ultrasonics Symp. Proc.*, 1994, pp. 607–610.

[4] P. Glynne-Jones, R. J. Boltryk, and M. Hill, "Acoustofluidics 9: Modelling and applications of planar resonant devices for acoustic particle manipulation," *Lab Chip*, vol. 12, pp. 1417–1426, 2012.

[5] J. J. Hawkes, R. W. Barber, D. R. Emerson, and W. T. Coakley, "Continuous cell washing and mixing driven by an ultrasound standing wave within a microfluidic channel," *Lab Chip*, vol. 4, no. 5, pp. 446–452, 2004.

[6] M. A. Grundy, W. T. Coakley, and D. J. Clarke, "Rapid detection of hepatitis-B virus using a hemagglutination assay in an ultrasonic standing wave field," *J. Clin. Lab. Immunol.*, vol. 30, no. 2, pp. 93–96, Oct. 1989.

[7] M. Gröschl, W. Burger, and B. Handl, "Ultrasonic separation of suspended particles—Part III: Application in biotechnology," *Acustica*, vol. 84, pp. 815–822, Sep.–Oct. 1998.

[8] C. M. Cousins, P. Holownia, J. J. Hawkes, M. S. Limaye, C. P. Price, P. J. Keay, and W. T. Coakley, "Plasma preparation from whole blood using ultrasound," *Ultrasound Med. Biol.*, vol. 26, no. 5, pp. 881–888, Jun. 2000.

[9] F. Petersson, A. Nilsson, C. Holm, H. Jonsson, and T. Laurell, "Separation of lipids from blood utilizing ultrasonic standing waves in microfluidic channels," *Analyst*, vol. 129, no. 10, pp. 938–943, 2004.

[10] N. R. Harris, M. Hill, R. J. Townsend, N. M. White, and S. P. Beeby, "Performance of a micro-engineered ultrasonic particle manipulator," *Sens. Actuators B*, vol. 111, no. 5485, pp. 481–486, 2005.

[11] S. P. Martin, R. J. Townsend, L. A. Kuznetsova, K. A. Borthwick, M. Hill, M. B. McDonnell, and W. T. Coakley, "Spore and micro-particle capture on an immunosensor surface in an ultrasound standing wave system," *Biosens. Bioelectron.*, vol. 21, no. 5, pp. 758–767, 2005.

[12] G. Goddard and G. Kaduchak, "Ultrasonic particle concentration in a line-driven cylindrical tube," *J. Acoust. Soc. Am.*, vol. 117, pp. 3440–3447, Jun. 2005.

[13] D. Bazou, G. A. Foster, J. R. Ralphs, and W. T. Coakley, "Molecular adhesion development in a neural cell monolayer forming in an ultrasound trap," *Mol. Membr. Biol.*, vol. 22, pp. 229–240, May–Jun. 2005.

[14] K. A. J. Borthwick, W. T. Coakley, M. B. McDonnell, H. Nowotny, E. Benes, and M. Gröschl, "Development of a novel compact sonicator for cell disruption," *J. Microbiol. Methods*, vol. 60, pp. 207–216, Feb. 2005.

[15] Y. H. Lee, J. O. You, and C. A. Peng, "Retroviral transduction of adherent cells in resonant acoustic fields," *Biotechnol. Prog.*, vol. 21, pp. 372–376, Mar.–Apr. 2005.

[16] J. Hultström, O. Manneberg, K. Dopf, H. M. Hertz, H. Brismar, and M. Wiklund, "Proliferation and viability of adherent cells manipulated by standing-wave ultrasound in a microfluidic chip," *Ultrasound Med. Biol.*, vol. 33, no. 1, pp. 145–151, 2007.

[17] H. Böhm, P. Anthony, M. R. Davey, L. G. Briarty, J. B. Power, K. C. Lowe, E. Benes, and M. Gröschl, "Viability of plant cell suspensions exposed to homogeneous ultrasonic fields of different energy density and wave type," *Ultrasonics*, vol. 38, pp. 629–632, Mar. 2000.

[18] Z. W. Wang, P. Grabenstetter, D. L. Feke, and J. M. Belovich, "Retention and viability characteristics of mammalian cells in an acoustically driven polymer mesh," *Biotechnol. Prog.*, vol. 20, pp. 384–387, Jan–Feb. 2004.

[19] S. Radel, A. J. McLoughlin, L. Gherardini, O. Doblhoff-Dier, and E. Benes, "Viability of yeast cells in well controlled propagating and standing ultrasonic plane waves," *Ultrasonics*, vol. 38, pp. 633–637, Mar. 2000.

[20] D. Bazou, R. Kearney, F. Mansergh, C. Bourdon, J. Farrar, and M. Wride, "Gene expression analysis of mouse embryonic stem cells following levitation in an ultrasound standing wave trap," *Ultrasound Med. Biol.*, vol. 37, pp. 321–330, Feb. 2011.
[21] O. Manneberg, B. Vanherberghen, B. Onfelt, and M. Wiklund, "Flow-free transport of cells in microchannels by frequency-modulated ultrasound," *Lab Chip*, vol. 9, no. 6, pp. 833–837, 2009.
[22] P. Glynne-Jones, R. J. Boltryk, N. R. Harris, A. W. J. Cranny, and M. Hill, "Mode-switching: A new technique for electronically varying the agglomeration position in an acoustic particle manipulator," *Ultrasonics*, vol. 50, pp. 68–75, Jan. 2010.
[23] A. Haake, A. Neild, G. Radziwill, and J. Dual, "Positioning, displacement, and localization of cells using ultrasonic forces," *Biotechnol. Bioeng.*, vol. 92, pp. 8–14, Oct. 5, 2005.
[24] Y. Abe, M. Kawaji, and T. Watanabe, "Study on the bubble motion control by ultrasonic wave," *Exp. Therm. Fluid Sci.*, vol. 26, pp. 817–826, Aug. 2002.
[25] C. R. P. Courtney, C. K. Ong, B. W. Drinkwater, P. D. Wilcox, C. Démoré, S. Cochran, P. Glynne-Jones, and M. Hill, "Manipulation of microparticles using phase-controllable ultrasonic standing waves," *J. Acoust. Soc. Am.*, vol. 128, pp. EL195–EL199, Oct. 2010.
[26] T. Kozuka, T. Tuziuti, H. Mitome, and T. Fukuda, "Control of a standing wave field using a line-focused transducer for two-dimensional manipulation of particles," *Jpn. J. Appl. Phys.*, vol. 37, pp. 2974–2978, May 1998.
[27] M. Hill and N. R. Harris, "Ultrasonic particle manipulation," in *Microfluidic Technologies for Miniaturized Analysis Systems*, S. Hardt and F. Schönfeld, Eds., New York, NY: Springer, 2007, pp. 357–392.
[28] L. V. King, "On the acoustic radiation pressure on spheres," *Proc. R. Soc. Lond. A*, vol. 147, no. 861, pp. 212–240, 1934.
[29] K. Yosioka and Y. Kawasima, "Acoustic radiation pressure on a compressible sphere," *Acustica*, vol. 5, no. 3, pp. 167–173, 1955.
[30] L. P. Gor'kov, "On the forces acting on a small particle in an acoustical field in an ideal fluid," *Sov. Phys. Dokl.*, vol. 6, no. 9, pp. 773–775, 1962.
[31] B. Hammarström, M. Evander, H. Barbeau, M. Bruzelius, J. Larsson, T. Laurell, and J. Nilsson, "Non-contact acoustic cell trapping in disposable glass capillaries," *Lab Chip*, vol. 10, no. 17, pp. 2251–2257, 2010.
[32] T. Lilliehorn, U. Simu, M. Nilsson, M. Almqvist, T. Stepinski, T. Laurell, J. Nilsson, and S. Johansson, "Trapping of microparticles in the near field of an ultrasonic transducer," *Ultrasonics*, vol. 43, pp. 293–303, Mar. 2005.
[33] P. Glynne-Jones, R. J. Boltryk, M. Hill, N. R. Harris, and P. Baclet, "Robust acoustic particle manipulation: A thin-reflector design for moving particles to a surface," *J. Acoust. Soc. Am.*, vol. 126, no. 3, pp. EL75–EL79, 2009.
[34] C. E. M. Démoré, J. A. Brown, and G. R. Lockwood, "Investigation of cross talk in kerfless annular arrays for high-frequency imaging," *IEEE Trans. Ultrason. Ferroelectr. Freq. Control*, vol. 53, no. 5, pp. 1046–1056, 2006.
[35] C. E. Morton and G. R. Lockwood, "Evaluation of kerfless linear arrays," in *Proc. IEEE Ultrasonics Symp.*, 2002, vol. 2, pp. 1257–1260.
[36] M. Hill, Y. Shen, and J. J. Hawkes, "Modelling of layered resonators for ultrasonic separation," *Ultrasonics*, vol. 40, no. 1–8, pp. 385–392, 2002.

Peter Glynne-Jones graduated from the School of Electronics and Computer Science at the University of Southampton, and was an IET scholar. His 2001 Ph.D., "Vibration powered generators for self-powered microsystems," led to the spin-off company Perpetuum. More recently, Peter has been involved in researching the manipulation of particles in microsystems using ultrasonic radiation forces, covering a range of topics from fundamental modeling of radiation forces and streaming, to manipulation, separation, and sorting devices. His current focus extends to the applications of ultrasonic radiation forces in biological assays and tissue engineering.

Christine E. M. Démoré (née Morton) received the B.Sc.E. degree in engineering physics and a Ph.D. degree in physics from Queen's University, Kingston, Canada, in 2000 and 2006, respectively. Following graduate work, Dr. Démoré moved to Scotland to pursue research in ultrasound for medicine and life sciences. Currently, she is a research fellow at the Institute for Medical Science and Technology, University of Dundee. Her research interests include the development of ultrasonic devices for applications including diagnostic imaging, medical intervention, and life sciences applications, including manipulation of particles and cells.

Congwei Ye graduated with an M.Sc. degree from the School of Engineering Science at the University of Southampton, and a B.Eng. degree from the School of Mechanical Engineering Science at Donghua University, China. Her master's thesis, "Ultrasonic field of cell trapping and manipulation microfluidic system," focused on using a transducer array to trap and manipulate mico-sized particles in a fluidic system. She is currently working as a project engineer at Air Products and Chemical (China) Inc.

Yongqiang Qiu graduated in biomedical engineering with a B.Eng. degree from Tianjin University, Tianjin, China, in 2007. He also received an M.Sc. degree in biomedical engineering from the University of Dundee, UK, in 2009. Currently, he is a Ph.D. student working on the development of ultrasonic devices for cell manipulation and characterization at the Institute for Medical Science and Technology, University of Dundee. His research interests include high-frequency ultrasonic transducer fabrication, finite element analysis (FEA), and cell manipulation technology.

Sandy Cochran is Professor of Biophysical Science and Engineering, and Team Leader in Medical Ultrasound, in the University of Dundee's Institute for Medical Science and Technology.

He received the B.Sc. degree in electronics and computing in 1986, the Ph.D. degree for work on ultrasonic arrays in 1990, and an M.B.A. degree for an investigation of universities as part of an enterprise network in 2001, all from the University of Strathclyde. His present research interests are focused on medical ultrasound devices, with applications in diagnosis, imaging, and therapy. He also maintains interest in relevant materials, systems design, and applications issues, and in underwater sonar and industrial processing for medical and life sciences applications. Outside work, he divides his time between his homes in Dundee and Glasgow.

Martyn Hill is Professor of Electromechanical Systems and Head of Engineering Sciences at the University of Southampton. Martyn was awarded a degree in engineering acoustics in 1985 from the Institute of Sound and Vibration Research at Southampton and then moved to the mechanical engineering department, where he carried out research into parameter estimation techniques for noninvasive biomedical measurement and the development of automotive sensors. He was appointed lecturer in 1990 and is now a Professor in the Electro-Mechanical Research Group. Martyn's principal research interest is the use and modeling of ultrasonic radiation forces, particularly their application in microfluidic systems, and in the manipulation of micrometer-scale particles and cells.